Composites Science and Technology 71 (2011) 535–540

Contents lists available at ScienceDirect

Composites Science and Technology

journal homepage: www.elsevier.com/locate/compscitech

Composites of polypropylene melt blended with synthesized silica nanoparticles

H. Palza [a,*], R. Vergara [a], P. Zapata [b]

[a] Departamento de Ingeniería Química y Biotecnología, Facultad de Ciencias Físicas y Matemáticas, Universidad de Chile, Beauchef 850, Santiago, Chile
[b] Grupo Polímeros, Facultad de Química y Biología, Universidad de Santiago, Av. Alameda Libertador B. O'Higgins 3363, Santiago, Chile.

ARTICLE INFO

Article history:
Received 16 August 2010
Received in revised form 22 December 2010
Accepted 5 January 2011
Available online 9 January 2011

Keywords:
A. Polymer–matrix composites (PMCs)
D. Thermogravimetric analysis (TGA)
B. Thermal properties

ABSTRACT

Spherical and layered silica nanoparticles synthesized by the sol–gel method were melt blended with a polypropylene matrix in order to quantify their effect on thermal and mechanical behaviours of the resulting polymer composites. Transmission electron microscopy images showed that spherical nanoparticles were dispersed in the polymer matrix whereas layered particles display tactoid and agglomerated structures. By thermogravimetric analysis, it was observed that independent of the particle aspect ratio, the nanofillers render larger thermal degradation stabilization to the polymer matrix under oxidative conditions than under inert atmosphere. Noteworthy, the largest improvements were found by using spherical nanoparticles in presence of a compatibilizer. These results allow the conclusion that the physical/chemical adsorption of the volatile products on the particle surface during the oxidative degradation is the plausible mechanism behind the thermal stabilization. Tensile stress–strain tests otherwise showed that composites with spherical nanoparticles can display similar or even larger elastic modulus than composites with layered particles showing that the polymer/particle entanglement could be the mechanism for the load transfer in these nanocomposites.

1. Introduction

It is well known today, although not completely understood, that nanoparticles can affect polymer properties such as: crystallization, mechanical strength, melt processing, electrical and thermal conductivity, and viscoelasticity, among others [1–7]. Two of the best examples of the above mentioned are the large thermal degradation stability and higher stiffness rendered to polymer matrices by adding small amounts of clay particles [1,2,8–15].

Either physical or chemical mechanisms have been reported regarding the enhanced thermal stability of polymer/clay nanocomposites. The chemically-related mechanisms are mainly based on structural metals present in the clay reacting with free radicals coming from the polymer degradation reactions [16,17]. Another explanation postulates the physical–chemical adsorption of the volatile degradation materials on the silicate layers delaying the process [13,18,19]. The physical models otherwise are based on the lower diffusivity that polymer/clay composites present due to the so called "labyrinth effect". The high aspect ratio of silicate layers reduces the out-diffusion of volatile decomposition products [20,21]. Under thermo-oxidative conditions, the presence of the high contact-area between the polymer and the filler could further hinder the penetration of oxygen molecules [11,18]. Another physical model recently published is related with the suppression of the molecular mobility of polymers surrounding the clay or being inside their galleries [11,21–24].

Despite the extensive research on thermal stability of clay nanocomposites a different approach should be developed overcoming its main limitations such as: presence of organic modifiers, several hierarchical/morphological clay structures in the nanocomposite, and presence of a compatibilizer and structural metals, among others [25]. One novel route is to use synthetic sol–gel nanoparticles as filler. The main advantages of sol–gel nanoparticles are the size and aspect ratio control of the particle and the absence of impurities [26]. Moncada et al. reported that the addition of spherical and layered nanoparticles synthesized by the sol–gel method increases the thermal stability of polypropylene under oxidative conditions in the presence of a compatibilizer [27]. Furthermore, our group has recently reported that the addition of spherical nanoparticles of ~70 nm can dramatically improve the thermal degradation of polypropylene under oxidative conditions [19]. Sol–gel based nanoparticles can further increase the mechanical properties of the polypropylene depending on its aspect ratio and presence of a compatibilizer [27–33]. Composites of polypropylene with 1 wt.% of silica nanospheres and 3 wt.% of compatibilizer display elastic modulus 40% higher than the neat matrix whereas layered sol–gel filler displays improvements as high as 70% [27]. Other authors have shown the positive effect of the surface modification of the nanosilica on the mechanical behaviour of polypropylenes [30–32].

In this contribution, polypropylene nanocomposites were prepared by using spherical and layered silica nanoparticles

* Corresponding author. Fax: +56 2 699 10 84.
E-mail address: hpalza@ing.uchile.cl (H. Palza).

0266-3538/$ - see front matter © 2011 Elsevier Ltd. All rights reserved.
doi:10.1016/j.compscitech.2011.01.002

synthesized by the sol–gel method and their thermal resistance, as quantified by thermogravimetric analysis (TGA), and mechanical properties under tensile conditions were analyzed.

2. Experimental

2.1. Synthesis of the spherical and layered silica nanoparticles

Spherical silica nanoparticles were synthesized by the sol–gel method using a two-stage mixed semi-batch method, as previously reported [34]. The hybrid layered silica nanoparticles were synthesized by the sol–gel method as described elsewhere [27]. 20 g of octadecylamine (ODA) acting as a template were dissolved in an ethanol (100 ml)/water (80 ml) mixture at 50 °C. Solid $NaNO_3$ (0.255 g) and $Al(NO_3)_3$ 9H2O (1.12 g) were then added to the surfactant solution, and a solution of TEOS (3.8 ml) in 50 ml of ethanol under nitrogen was poured into the clear surfactant solution. After several minutes, a white precipitate was formed. These particles were characterized by X-ray diffraction where a peak at $2\theta = 2.2°$ was observed confirming the regular layered structure of the particles with an interlayer distance of 4 nm.

2.2. Preparation of the polypropylene nanocomposites

A polypropylene homopolymer (PP) from Petroquim (Chile) with a melt flow rate of 3 g/10 min was used as the polymeric matrix. The composites were prepared by using a Brabender plasticorder internal mixer at 190 °C and a speed of 110 RPM during 10 min. Predetermined amounts of the silica nanoparticles, antioxidant and neat polymer were mixed under nitrogen atmosphere in order to obtain nanocomposites with 1, 3, 5 w/w% of nanofiller. A commercial polypropylene grafted with maleic anhydride from Aldrich (PP-g-MA) with 0.6 mol% content was used as compatibilizer. In this case, a master batch containing a mixture of silica nanoparticles and the compatibilizer with a weight ratio of 1:3 was prepared.

2.3. Nanocomposite characterization

Thermogravimetric analysis (TGA) was carried out under either nitrogen or air by using a Netzsch TG 209 F1 Iris equipment from room temperature to 600 °C at a heating rate of 20 °C/min. The gas flow rate was stated in 100 ml/min independent of the sample weight that was in the range of 5–10 mg. Several measurements were carried out for the pure polymer in order to evaluate the standard deviation of TGA. In these measurements the experimental error was about 2% that it can be extrapolated to the other samples. Therefore, changes in more than 15 °C between samples can be considered as significantly different by for example the ANOVA analysis. Images coming from high-resolution transmission electron microscopy (HRTEM) were taken in a FEI microscope model G2 F20 S-Twin at 200 kV. Ultrathin sections of about 70 nm were obtained by cutting the samples with an Ultracut Reichert-Jung microtome equipped with a Diatome diamond knife. The mechanical properties were measured using a HP D500 dynamometer at a rate of 50 mm/min at 23 °C and 30% relative humidity. The samples were press molded at 190° C with 50 bar of pressure for 5 min and cooled under pressure by flushing the press with cold water. A minimum of three samples were tested for each material and the average values are reported. The experimental error was about 6% relative to the mean value as displayed in Fig. 6.

3. Results

3.1. Morphological characterization of nanocomposites

Fig. 1 displays some representative images of the different nanocomposites studied. Spherical silica particles (SSP) with sizes ranging from 50 nm to 110 nm are mainly observed. These

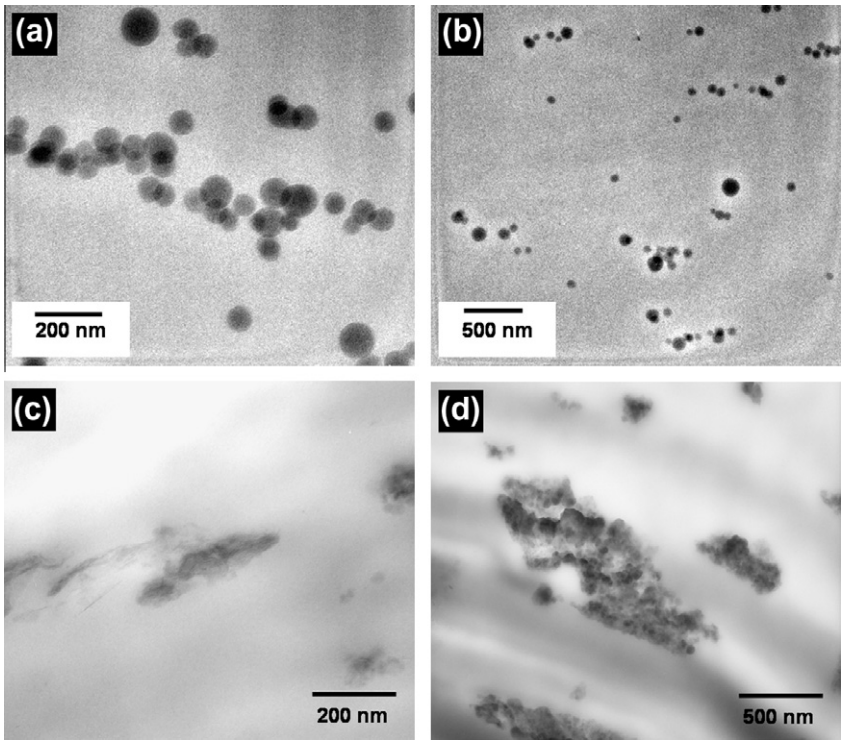

Fig. 1. Representative TEM images of the nanocomposites studied by using spherical (Fig. 1a and b) and layered (Fig. 1c and d) filler nanoparticles in presence of a compatibilizer.

particles are rather dispersed in the polymeric matrix especially when the compatibilizer is used as displayed in Fig. 1b for composites with 5 wt.% of filler. In general, two particle structures are recognized in the filled matrix: 1) well dispersed and semi-isolated single particles (Figs. 1b and 2)) weakly agglomerated particles with complex cluster structures formed by a few particles, as observed in Fig. 1a. It is highlighted that these spherical particles present three relevant differences compared with typical clay nanoparticles: 1) the sol–gel method produces extremely highly pure materials; 2) an aspect ratio (1) that is about 300 times lower than exfoliated or intercalated clays; and 3) there are not any organic molecules in these nanoparticles.

A different behaviour is observed for layered silica particles (LSP) as displayed in Fig. 1c and d. A fraction of these particles are poorly dispersed in the polymer matrix and large aggregates can be observed representing tactoid structures similar to some natural clay particle composites. Nevertheless, together with these tactoid structures is possible to observe particles in intercalated or exfoliated states as in Fig. 1c. This complex morphology is confirmed by X-ray diffractions (results not shown) as the d_{001} diffraction peak, related with the gap distance between layers, is not modified in the nanocomposites. This effect is not significantly affected by the presence of the compatibilizer. Similar results has been shown in synthetic layered silica particles melt blended with polystyrene where platelet stacks and flocculated particles were mainly observed by TEM [35].

3.2. Non-oxidative thermal stability

Fig. 2 displays the effect of adding 5 wt.% of nanoparticles on the thermal degradation of the polypropylene under inert conditions as measured by thermogravimetric analysis (TGA). In this condition, the nanoparticles slightly affect the thermal behaviour although the whole degradation process is narrowed in the nanocomposites. The onset temperature of degradation (T_{onset}) is increased with differences as high as 35 °C relative to the pure polymer. The T_{peak} is decreased ~10 °C in nanocomposites with LSP as previously observed in some polypropylene/clay nanocomposites [11,15,36,37]. Although this difference can be associated with the experimental error, values under oxidative conditions confirm that it is a general behaviour as discussed below. In our case, the degradation of the organic template used in LSP can catalyze the polymer degradation explaining the decrease in T_{peak} [11,15,36,37]. To verify this hypothesis, TGA was carried out to the layered particles observing that the ODA degradation is characterized for a T_{onset} of 180 °C confirming that its degradation could explain our findings. The presence of a compatibilizer otherwise is able to slightly improve the thermal degradation of the composites as displayed in Fig. 2. For LSP the presence of the compatibilizer shifts the degradation processes to higher temperatures and the T_{peak} increases 15 °C becoming higher than the pure sample. Noteworthy, the composites with SSP display a narrower degradation process when the compatibilizer is used. These results can be associated with a better dispersion of the nanoparticles when the compatibilizer is added to the system [27,29].

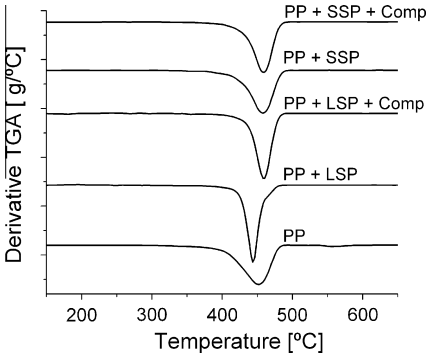

Fig. 2. Derivative TGA for the different polypropylene composites with 5 wt.% of particles under inert atmosphere. LSP: layered silica particle, SSP: spherical silica nanoparticle; and Comp: compatibilizer.

Figs. 3 and 4 summarize the effect of the filler content on the thermal behaviour of the nanocomposites for the different particles showing further the effect of the compatibilizer. Regarding to T_{onset}, its increase reaches a plateau at concentrations approximately 3 wt.% as a high amount of nanoparticles can induce agglomeration processes. By adding the compatibilizer, a higher T_{onset} is obtained, especially at low filler content, because of the better particle dispersion. There is not any relevant effect of the filler content on the T_{peak} as observed in Fig. 4 independent of the filler aspect ratio and of the compatibilizer. The only relevant change is for the highest amount of LSP as above discussed.

3.3. Oxidative thermal stability

A larger effect of the nanoparticles on the polymer degradation behaviour is observed under oxidative conditions as displayed in Fig. 5 for composites with 5 wt.% of filler [38]. By adding nanoparticles the T_{peak} is dramatically shifted to higher values and differences as high as 70 °C are observed. Furthermore, the whole degradation process is broadened instead of narrowed as under inert conditions. The presence of a compatibilizer otherwise improves the thermal stabilization as measured by T_{peak}. Noteworthy, the best results are obtained by using SSP with the compatibilizer. Nanocomposites with LSP present lower T_{onset} than the neat sample independent of the presence of a compatibilizer. For SSP fillers

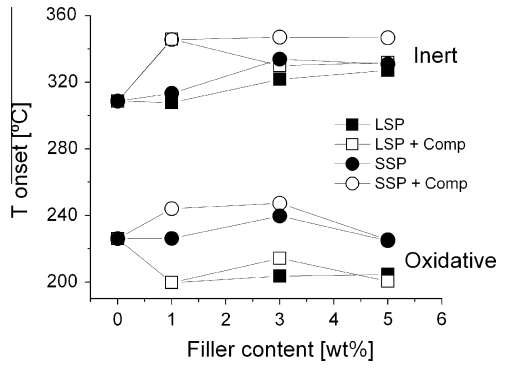

Fig. 3. Effect of the particle content and presence of a compatibilizer on the on-set temperature of degradation (T_{onset}) as measured by TGA under inert and oxidative conditions.

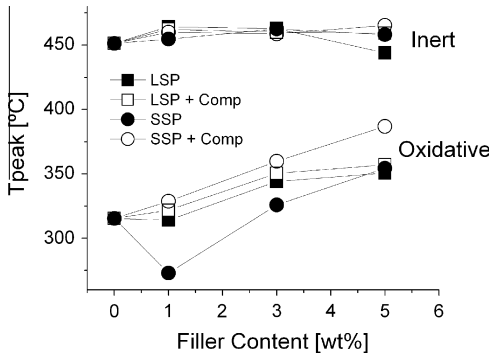

Fig. 4. Effect of the particle content and presence of a compatibilizer on the maximum weight loss rate temperature of degradation (T_{peak}) as measured by TGA under inert and oxidative conditions.

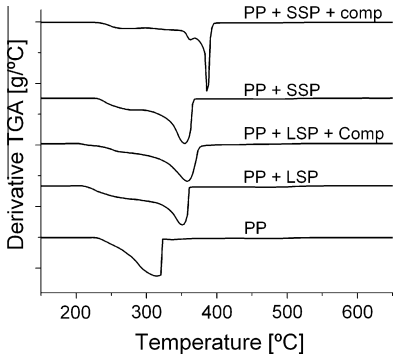

Fig. 5. Derivative TGA for the different polypropylene composites with 5 wt.% of particles under oxidative conditions. LSP: layered silica particle, SSP: spherical silica nanoparticle; and Comp: compatibilizer.

otherwise, T_{onset} is not dramatically altered confirming that the behaviour of LSP based composites is owing to the organic templates acting as catalysts for the thermal degradation of the polymer.

Regarding the filler content, Figs. 3 and 4 display the effect of the nanoparticle concentration on T_{onset} and T_{peak}, respectively. From Fig. 3, it is confirmed that LSP systematically and significantly render lower degradation temperatures than the pure polymer because of the presence of the organic template in the whole range of filler concentration studied. This behaviour is independent of the presence of the compatibilizer. On the other hand, it seems that T_{onset} temperatures are independent of the filler concentration, although more points are needed in order to confirm this trend by a statistical approach. By comparing Figs. 3 and 4, it is possible to conclude that under oxidative condition, the effect of the particles is stronger in T_{peak} than in T_{onset} in all nanocomposites. Fig. 4 further shows that, by increasing the filler content, it is possible to obtain higher T_{peak} and the composite prepared with the highest amount of SSP using the compatibilizer displays larger thermal stabilization than those based on LSP.

3.4. Mechanical properties

Fig. 6 displays a summary of the effect of the particle aspect ratio, filler concentration, and presence of a compatibilizer on the elastic modulus of the composites. Similar to the thermal degradation behaviour, the highest values in the elastic strength are obtained by using SSP, even considering the experimental error.

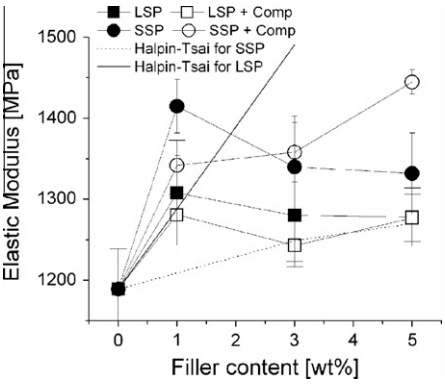

Fig. 6. Effect of the filler content and presence of a compatibilizer on the elastic modulus (from tensile stress–strain tests) of the nanocomposites. The larger capwidth from the standard deviations represents the values from LSP. Solid and doted lines represent the theoretical results from layered and spherical filler respectively, as estimated from the Halpin–Tsai model (Eq. (1)).

Noteworthy, 1 wt.% of SSN increases the elastic modulus in approximately 20% although at higher filler concentrations the property slightly decreases probably because of agglomeration processes. By improving the dispersion of the SSP with the compatibilizer, the increase in the mechanical elasticity becomes proportional to the filler content owing to better dispersion reaching the highest value with 5 wt.% of SSP. Fig. 6 confirms that the compatibilizer does not improve the performance of composites based on LSP. Improvements of about 20% in the elastic modulus have been previously reported in composites of polyolefins with pure and surface modified spherical silica nanoparticles [1,28,29,32,39].

3.5. Discussion

Our main results from polypropylene composites with sol–gel nanoparticles of different aspect-ratio can be summarized as: (1) TGA results show that under oxidative conditions the nanocomposites display a much larger improvement in T_{peak} than under inert atmosphere that is even more drastic for SSP; and (2) composites with SSN present higher elastic modulus than LSP. These results can open up relevant information about the effect of the nanoparticle on the polymer performance as below discussed.

The fact that under oxidative conditions the nanocomposites present a much larger improvements in T_{peak} than under inert atmosphere means that the presence of oxygen should be considered in the mechanism behind thermal stability. Moreover, this difference between oxidative and inert conditions allows us to minimize the theory explaining the thermal stability because of the lower diffusion (or higher tortuosity) of the polymer degradation products as this mechanism applies under both atmospheres. The decrease of the oxygen diffusion from the outside region (gas phase) toward the polymer bulk can be ruled out as the initial thermal degradation processes are not strongly affected by the presence of the nanoparticles. Moreover, as recently reported [19], all mechanisms claiming the lower gas diffusion owing to nanoparticles in polymer composites are based on the high aspect ratio of the filler [40]. In theory, spherical particles do not modify the permeability or the diffusion of the matrix whereas layered fillers can drastically decrease it [19,40]. But our results show that SSN (aspect-ratio ~1) render the largest thermal improvements as measured by T_{peak}. Furthermore, sol–gel based particles do not present impurities able to react with the degradation products by the trapping mechanism ruling out this theory.

Based on the above mentioned, the physical/chemical adsorption of the volatile products on the particle surface during the oxidative degradation, which are different compounds as compared from those under inert atmosphere, can be a plausible mechanism behind better thermal stabilization of nanocomposites. Oxygen at high temperatures reacts with the polymer chains producing peroxide molecules, macro-radicals, oxidative dehydrogenation chains, oxidized volatile products, unsaturated hydrocarbons, alcohols, ketones, esters, etc. [38]. These oxidative degradation products are highly polar volatile molecules that can be easily adsorbed on the hydroxyl and other functional groups from the surface of the silica nanoparticles [41]. It is stressed that although SSP present the lowest aspect-ratio they have a high specific surface area (~70 m^2/g) that is larger than LSP (~44 m^2/g). Moreover, LSP are not well dispersed in the polymer matrix as observed in Fig. 1; therefore, its effective aspect ratio is low relative to the well dispersed natural clay particles. The latter explaining why SSP display the highest thermal stabilization as measured by T_{peak} by using a compatibilizer as a higher area is available for the adsorption. In this context, the effect of the filler content can be understood as a complex phenomenon involving two opposite processes as more particles implies more area adsorbing the degradation products but also implies higher probability of aggregation.

Moreover, the presence of a compatibilizer decreases the probability of agglomeration having as consequence larger changes in the properties with the filler content, especially by using SSP.

It is highlighted that nanocomposites prepared with the same polypropylene matrix but using natural clay particles with good dispersion display larger thermal stability than our composites [14]. Therefore, adsorption of volatile products is one of the mechanisms explaining the thermal improvements but the "labyrinth" effect should be further considered when high aspect-ratio fillers are used.

Regarding the discussion about the mechanical properties of the nanocomposites, we used the Halpin–Tsai model to evaluate the effect of the filler on the relative elastic modulus of the composite relative to the pure matrix by [42]:

$$\frac{E_c}{E_m} = \frac{1 + 2 \cdot (L/t) \cdot f_p \cdot \eta}{1 - f_p \cdot \eta} \quad (1)$$

$$\eta = \frac{(E_p/E_m) - 1}{(E_p/E_m) + 2 \cdot (L/t)} \quad (2)$$

where f_p is the particle volume fraction; L/t is its aspect ratio (~10 and 1 for LSP and SSP, respectively); E_p and E_m are the longitudinal stiffness for the particle and matrix, respectively; and E_c is the longitudinal elastic modulus of the composite. For composites with SSP, the above mentioned equations can be directly applied by assuming a particle stiffness of 400 GPa [43]. Fig. 6 displays the values from Eq. (1) showing that this model systematically estimates lower values than the experimental ones. These results are rather confused considering that the Halpin–Tsai model should display higher values than the experimental results as it assumes perfect adhesion between the particle and the polymer. This assumption is not chemically plausible in our case even under the presence of a compatibilizer due to the strong non-polarity of polypropylene relative to the silica particles.

For polymer/layered particle nanocomposites the modification of some parameters accounting for its complex morphology is needed [42,43]:

$$\frac{L}{t} = \frac{L}{(N-1) \cdot d_{001} + d_s} \quad (3)$$

$$E_p = \frac{N}{t} \cdot E_s \cdot d_s \quad (4)$$

where L is the clay lateral size (250 nm); t is the particle thickness; E_s is the silica stiffness (400 GPa); d_s and d_{001} are the thickness of individual clay sheets (~1 nm) and the interlayer distance (~4 nm as measured by X-ray); N is the number of layers per stack supposed equal for all samples for simplicity (~20 units measured roughly by TEM). By taking account the above mentioned data coming from layered particles poorly dispersed in the polymer matrix, the Halpin–Tsai model predicts composites with dramatic increases in the elastic modulus with values as high as 1700 MPa at 5 wt.% of LSP whereas the experimentally values are ~1300 MPa. Noteworthy, the model states that LSP fillers are much effective increasing the mechanical elastic response of the matrix than SSP, this fact is not observed from our results.

The above mentioned results cannot be explained by the traditional concept of load transfer from the matrix to the particle by means of a perfect adhesion. Moreover, the nanoconfinement of the polymer matrix is not valid in our samples as the particle–particle distance is much higher than the polymer size as observed in Fig. 1 and predicted by theoretical models [19]. An alternative approach able to explain our results is the entanglement of the polymer chains with the nanospheres allowing the load transfer and increasing the stiffness of the chains that surround the particles. Actually, the average diameter of our polypropylene matrix is ~60 nm that is comparable to the average diameter of the spherical particles (~70 nm) [19]. This mechanism has been previously reported for single wall nanotubes [44] and nanospheres [45] but it is not valid for layered particles because of the large lateral size (Fig. 1) explaining the larger elastic modulus of composites based on SSP.

4. Conclusions

Our results from polypropylene composites based on sol–gel nanoparticles with different aspect ratio allow relevant conclusions toward the understanding of the behaviour of polymer nanocomposites. Samples prepared with SSP can display similar or even larger thermal stabilizations than those prepared with LSP under oxidative conditions showing that theories based on metallic impurities and lower diffusion of volatile products are not plausible. Because of the high specific area of the SSP, the chemical/physical adsorption of the polar volatile compounds from the oxidative degradation is the plausible mechanism explaining our results. In general, there is not a relevant effect of the filler content on the thermal degradation owing to filler agglomeration processes except in T_{peak} under oxidative conditions increasing with the particle content. Regarding the mechanical behaviour, SSP fillers can render similar or higher stiffness than LSP showing that the mechanism for the mechanical reinforcement is, probably, the entanglements of polymer chains surround the nanoparticles and not the standard load transfer by adhesion mechanism. In composites without the compatibilizer the largest effect is observed at 1 wt.% of filler as at higher concentrations the agglomeration processes avoid further reinforcements to the composite. Nevertheless, SSP particles in presence of the compatibilizer render an almost linear increase in the elastic modulus.

Acknowledgments

The authors gratefully acknowledge the financial support of CONICYT, projects FONDECYT INICIACION EN INVESTIGACION 11075001 and FONDECYT 1100058. It is also expressed the thanks to Dr. W. Sierralta for the TEM images and to Dr. R. Quijada for the support during this research.

References

[1] Ray S, Okamoto M. Polymer/layered silicate nanocomposites: a review from preparation to processing. Prog Polym Sci 2003;28:1539–641.
[2] Paul DR, Robeson LM. Polymer nanotechnology: nanocomposites. Polymer 2008;49:3187–204.
[3] Moniruzzaman M, Winey KI. Polymer nanocomposites containing carbon nanotubes. Macromolecules 2006;39:5194–205.
[4] Jeon K, Lumata L, Tokumoto T, Steven E, Brooks J, Alamo R. Low electrical conductivity threshold and crystalline morphology of single-walled carbon nanotubes – high density polyethylene nanocomposites characterized by SEM, Raman spectroscopy and AFM. Polymer 2007;48:4751–64.
[5] Usuki A, Kojima Y, Kawasumi M, Okada A, Fukusihima Y, Kurauchi TT. Synthesis of nylon 6-clay hybrid. Mater Res 1993;8:1179–84.
[6] Palza H, Reznik B, Kappes M, Hennrich F, Naue IFC, Wilhelm M. Characterization of melt flow instabilities in polyethylene/carbon nanotube composites. Polymer 2010;51:3753–61.
[7] Palza H, Gutiérrez S, Delgado K, Salazar O, Fuenzalida V, Avila J, et al. Toward tailor-made biocide materials based on polypropylene/copper nanoparticles. Macromol Rapid Commun 2010;31:563–7.
[8] Podsiadlo P, Kaushik AK, Arruda AM, Waas AM, Shim BS, Xu J, et al. Ultrastrong and stiff layered polymer nanocomposites. Science 2007;318:80–3.
[9] Liff SM, Kumar N, Mckinley GH. High-performance elastomeric nanocomposites via solvent-exchange processing. Nat Mater 2007;6:76–83.
[10] Manias E. Nanocomposites – Stiffer by design. Nat Mater 2007;6:9–11.
[11] Leszczynska A, Njuguna J, Pielichowski K, Banerjee JR. Polymer/montmorillonite nanocomposites with improved thermal properties. Part II. Thermal stability of montmorillonite nanocomposites based on different polymeric matrices. Therm Acta 2007;454:1–22.
[12] Guo B, Jia D, Cai C. Effects of organo-montmorillonite dispersion on thermal stability of epoxy resin nanocomposites Eur. Polym J 2004;40:1743–8.

[13] Qin H, Zhang S, Zhao C, Feng M, Yang M, Shu Z, et al. Thermal stability and flammability of polypropylene/montmorillonite composites. Polym Degrad Stabil 2004;85:807–13.
[14] Palza H, Yazdani-Pedram M. Effect of the hierarchical structure in poly(propylene)/clay composites on their thermal stability: from single- to multi-step degradation processes. Macromol Mater Eng 2009;295:48–57.
[15] Leszczynska A, Njuguna J, Pielichowski K, Banerjee JR. Polymer/montmorillonite nanocomposites with improved thermal properties. Part I. Factors influencing thermal stability and mechanisms of thermal stability improvement. Therm Acta 2007;453:75–96.
[16] Solomon DH, Swif JD. Reactions catalyzed by minerals. II. Chain termination in free-radical polymerizations.. J Appl Polym Sci 1967;11:2567–75.
[17] Zhu J, Uhl FM, Morgan AB, Wilkie CA. Studies on the mechanism by which the formation of nanocomposites enhances thermal stability. Chem Mater 2001;13:4649–54.
[18] Zanetti M, Camino G, Reichert R, Mulhaupt R. Thermal behaviour of poly(propylene) layered silicate nanocomposites. Macromol Rapid Commun 2001;22:176–80.
[19] Palza H, Vergara R, Zapata P. Improving the thermal behaviour of polypropylene by addition of spherical silica nanoparticles. Macromol Mater Eng 2010;295:899–905.
[20] Gilman JW, Jackson CL, Morgan AB, Harris R, Manias E, Giannelis EP. Flammability properties of polymer – Layered-silicate nanocomposites. Polypropylene and polystyrene nanocomposites. Chem Mater 2000;12:1866–73.
[21] Chen K, Vyazovkin S. Mechanistic differences in degradation of polystyrene and polystyrene-clay nanocomposite: Thermal and thermo-oxidative degradation. Macromol Chem Phys 2006;207:587–95.
[22] Chen K, Wilkie CA, Vyazovkin S. Nanoconfinement revealed in degradation and relaxation studies of two structurally different polystyrene-clay systems. J Phys Chem B 2007;111:12685–92.
[23] Chen K, Susner MA, Vyazovkin S. Effect of the brush structure on the degradation mechanism of polystyrene-clay nanocomposites. Macromol Rapid Commun 2005;26:690–5.
[24] Blumstein A. Polymerization of adsorbed monolayers II: thermal degradation of the inserted polymer. J Appl Sci Part A 1965;3:2665–72.
[25] Pandey JK, Reddy KR, Kumar AP, Singh RP. An overview on the degradability of polymer nanocomposites. Polym Degrad Stabil 2005;88:234–50.
[26] Hench LL, West JK. The sol–gel process. Chem Rev 1990;90:33–72.
[27] Moncada E, Quijada R, Retuert J. Nanoparticles prepared by the sol–gel methos and their use in the formation of nanocomposites with polypropylene. Nanotechnology 2007;18:335606.
[28] Liu Y, Kontopoulou M. The structure and physical properties of polypropylene and thermoplastic olefin nanocomposites containing nanosilica. Polymer 2006;47:7731–9.
[29] Zoukrami F, Haddaoui N, Vanzeveren C, Sclavons M, Devaux J. Effect of compatibilizer on the dispersion of untreated silica in a polypropylene matrix. Polym Int 2008;57:756–63.
[30] Wu CL, Zhang MQ, Rong MZ, Friedrich K. Silica nanoparticles filled polypropylene: effects of particle surface treatment, matrix ductility and particle species on mechanical performance of the composites. Compos Sci Technol 2005;65:635–45.
[31] Bikiaris DN, Papageorgiou GZ, Pavlidou E, Vouroutzis N, Palatzoglou P, Karayannidis GP. Preparation by melt mixing and characterization of isotactic polypropylene/SiO_2 nanocomposites containing untreated and surface-treated nanoparticles. J Appl Polym Sci 2006;100:2684–96.
[32] Rong MZ, Zhang MQ, Zheng YQ, Zeng HM, Walter R, Friedrich K. Structure–property relationships of irradiation grafted nano-inorganic particle filled polypropylene composites. Polymer 2001;42:167–83.
[33] Vladimirov V, Betchev C, Vassiliou A, Papageorgiou G, Bikiaris D. Dynamic mechanical and morphological studies of isotactic polypropylene/fumed silica nanocomposites with enhanced gas barrier properties. Compos Sci Technol 2006;66:2935–44.
[34] Kim K, Kim HJ. Formation of silica nanoparticles by hydrolysis of TEOS using a mixed semi-batch/batch method. J Sol–Gel Sci Technol 2002;25:183–9.
[35] Chastek TT, Stein A, Macosko C. Hexadecyl-functionalized lamellar mesostructured silicates and aluminosilicates designed for polymer–clay nanocomposites. Part II: dispersion in organic solvents and in polystyrene. Polymer 2005;46:4431–9.
[36] Tang Y, Hu Y, Song L, Zong R, Gui Z, Chen Z, et al. Preparation and thermal stability of polypropylene/montmorillonite nanocomposites. Polym Degrad Stabil 2003;82:127–31.
[37] Tidjani A, Wald O, Pohl MM, Hentschel MP, Schartel S. Polypropylene-graft-maleic anhydride-nanocomposites: I – characterization and thermal stability of nanocomposites produced under nitrogen and in air. Polym Degrad Stabil 2003;82:133–40.
[38] Gianelli W, Ferrara G, Camino G, Pellegatti G, Rosenthal J, Tromboni RC. Effect of matrix features on polypropylene layered silicate nanocomposites. Polymer 2005;46:7037–46.
[39] Kontou E, Niaounakis M. Thermo-mechanical properties of LLDPE/SiO_2 nanocomposites. Polymer 2006;47:1267–80.
[40] Gusev AA, Lusti HR. Rational design of nanocomposites for barrier applications. Adv Mater 2001;13:1641.
[41] Zou H, Wu S, Shen J. Polymer/silica nanocomposites: preparation, characterization, properties, and applications. Chem Rev 2008;108:3893–957.
[42] Sheng N, Boyce MC, Parks DM, Rutledge GC, Abes JI, Cohen RE. Multiscale micromechanical modeling of polymer/clay nanocomposites and the effective clay particle. Polymer 2004;45:487–506.
[43] Fornes TD, Paul DR. Modeling properties of nylon 6/clay nanocomposites using composite theories. Polymer 2003;44:4993–5013.
[44] Mu M, Winey KI. Improved load transfer in nanotube/polymer composites with increased polymer molecular weight. J Phys Chem C 2007;111:17923–7.
[45] Sternstein SS, Zhu AJ. Reinforcement mechanism of nanofilled polymer melts as elucidated by nonlinear viscoelastic behavior. Macromolecules 2002;35:7262–73.